Johnson Noise and Shot Noise Determinations of k_B, T_0, and e

Bhaskar Mookerji and Charles Herder*
MIT Department of Physics, 8.13
(Dated: March 6, 2008)

We examine voltage noise arising from two stochastic processes in electrical systems. We verify Nyquist's theorem of voltage noise by measuring the amplified Johnson noise across a series of coaxial-lead metal film resistors at a variety of temperatures, yielding Boltzmann's constant $k_B = (1.38 \pm 0.06) \times 10^{-23} \mathrm{J} \cdot \mathrm{K}^{-1}$ and absolute zero $T_0 = (-263.49 \pm 35.0 \pm 20.2)^{\circ}\mathrm{C}$. By characterizing the shot-nose across a photodiode, we find the electron charge $e = (1.59 \pm 0.08) \times 10^{-19}\mathrm{C}$.

1. INTRODUCTION

Unwanted electrical fluctuations—noise—found in signals interferes with measurement accuracy and precision. Noise sources such as stray radio-frequency can be controlled, while others arise from physically-inherent stochastic fluctuations. Johnson noise quantifies the minimum mean-square voltage noise measurable from a signal source with a resistive impedance. Electric charge quantization and its resulting current fluctuations gives rise to shot noise[1].

We describe Johnson and shot noise as stochastic fluctuations in a resistor. To confirm Nyquist's Theorem, we measured an amplified passband of the Johnson noise power spectrum using a variety of resistors, from which Boltzmann's constant k_B and absolute zero T_0 are determined. The Butterworth frequency response of the amplification stage is characterized. We will also determine electron charge e from the shot noise current fluctuations through a photodiode[2].

2. THEORY

We investigate the noise voltage across a resistive impedance arising from the random thermal motions of its electrons. Noise can be represented by the spectral density $J_+(\omega)$ associated with a stochastically-fluctuating emf $V(t)$[3]:

$$\langle V^2 \rangle = \int_0^\infty d\omega J_+(\omega). \tag{1}$$

The spectral density is calculated by treating a resistor R_0 as an ideal, one-dimensional transmission line with characteristic impedance equal to R_0, operating at thermal equilibrium with temperature T. From the mean energy of a voltage wave propagating with frequency mode ω in the transmission line, we have

$$J_+(\omega) = \frac{2}{\pi} \frac{\hbar\omega}{e^{\hbar\omega/k_B T} - 1} R(\omega), \tag{2}$$

where $R(\omega)$ is the effective resistance seen by R_0 when accounting for a shunt capacitance C:

$$R(\omega) = \mathrm{Re}\left(R_0 || Z_C\right) = \frac{R_0}{1 + (\omega R_0 C)^2}. \tag{3}$$

In the high thermal limit with $\hbar\omega \ll k_B T$, the RHS Equation 2 simplifies to $(2/\pi) k_B T R(\omega)$, and we recover Nyquist's Theorem for the thermal noise across an impedance with a resistive part:

$$\langle V^2 \rangle = \frac{2 k_B T}{\pi} \int_0^\infty d\omega R(\omega) |Y(\omega)|^2, \tag{4}$$

where $|Y(\omega)|$ is voltage transfer function accounting for signal gain and bandpass filtering needed to measure micro-volt noise. We are interested in measuring this noise to determine k_B.

2.1. Shot Noise

Independent of thermal fluctuations, another source of stochastic noise follows from the quantization of electric charge. In this experiment's photodiode circuit, photo-excitation of electrons from a cathode creates a superposition of current events, each equal in magnitude to its electric charge e, flowing to an anode.

Assuming that electron arrivals at a rate K are independent of each other and therefore form a Poisson process, the time-average of fluctuating current is given by $\langle I \rangle = Ke$, and the average number of arrivals and variance for a random variable n in time interval τ is given by $K\tau$. From Poisson statistics, the shot noise current is given by

$$\langle I^2 \rangle = \langle \Delta I^2 \rangle = \frac{e\langle I \rangle}{\tau} \tag{5}$$

Applying Ohm's law across a resistor R_0 and relating the average time interval τ to the filter bandpass, we have

$$V_0^2 = \frac{e R_0^2 \langle I \rangle}{\pi} \int_0^\infty d\omega |Y(\omega)|^2. \tag{6}$$

3. EXPERIMENTAL SETUP AND PROCEDURE

Block diagrams depicting the Johnson and shot noise experiments can be found in Figures 1 and 2. Relevant

*Electronic address: mookerji@mit.edu, cherder@mit.edu

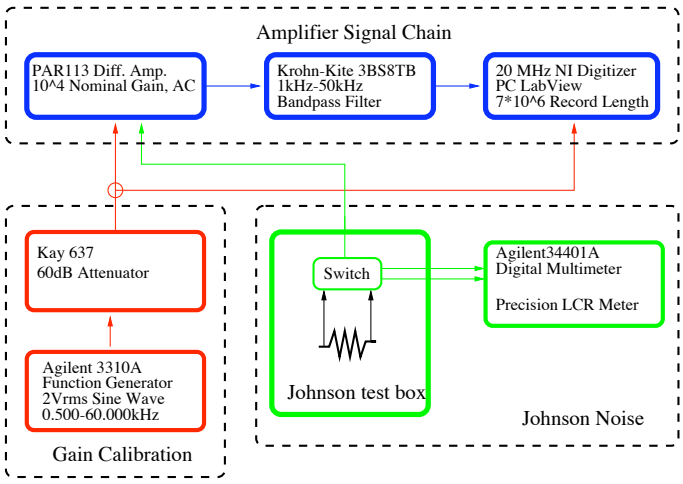

FIG. 1: Johnson noise and calibration apparatus for a fixed temperature and resistance. To increase precision in its signal averaging, the digitizer operates at the maximum 20MHz signal integration and a $7 \cdot 10^6$ sample record length. Household aluminum foil shields twisted, low-impedance coax cabling and the test box. The shield, test box, and amplifier are connected to grounding cable.

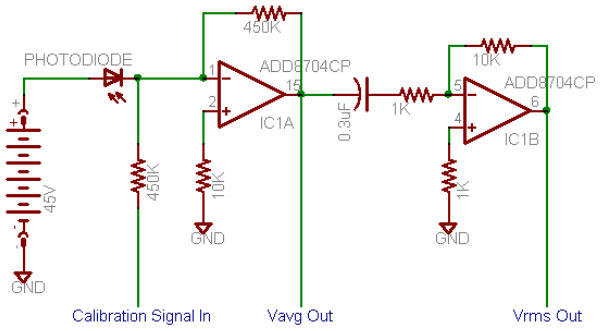

FIG. 2: Shot noise photodiode schematic. Voltage output from this stage is a measure of average current through a photodiode.

parameters applicable to both experiments are discussed in detail with respect to the Johnson noise measurement, followed by a discussion of the shot noise experiment.

3.1. Johnson Noise

We measure the voltage noise and resistances across eight axial-lead, metal film resistors (50kΩ to 800kΩ) mounted in alligator clips on a shielded aluminum test box connected to an amplifier stage. These measurements are repeated at thermal equilibrium with liquid nitrogen (77K), room-temperature ambient air (297.15K), and ambient air (393.15K) heated by a 120V AC Variac-controlled oven. It was not possible to measure the resistor's temperature directly without introducing additional voltage noise and capacitive coupling, therefore temperature was measured in the ambient media of the resistor's immediate vicinity using a toluene-filled glass thermometer and a digital thermometer. Resistance and capacitance measurements at low temperatures were taken quickly to inhibit capacitive charging. Lastly, frequency response for the gain calibration (Section 4.1) is given by the ratio of output and input RMS voltage for the amplifier stage over a 0.500-60.000kHz logarithmic sweep. We determine Boltzmann's constant and an absolute temperature scale with a re-expression of Equation 4,

$$\langle V^2 \rangle = 4 k_B R_0 T G, \tag{7}$$

where G is the effective noise bandwidth for a resistive impedance $R(\omega)$.

Accurately measuring thermal noise require that voltage and current noise in the amplifier, ambient electrical interference, and parasitic and shunt capacitance be minimized and accounted for. To determine amplifier noise, imagine an ideal, noise-free amplifier in series with imaginary voltage and current sources at its input. The amplifier is battery-powered to minimize 60Hz line noise, and source resistances are deliberately chosen to minimize additional noise through the amplifier. Shorting the resistor leads on the test box yields background voltage noise V_S in the amplifier chain. Assuming that sources of voltage noise are statistically uncorrelated, measured Johnson noise is given by $V^2 = V_R^2 - V_S^2$, where V_R^2 is the measured noise across a resistor. Measured background voltage obtained in this manner consistently fell between 11-13mV$_{\mathrm{RMS}}$ for all temperatures, while voltage across the resistor ranged between 70-100mV$_{\mathrm{RMS}}$ (at 393.15K)[4].

Ambient electrical interference and stray capacitance are minimized through proper grounding, additional shielding, and the use of low impedance cabling. Using the LCR meter on the multimeter ports on the test box, we measure for each resistor the capacitance of coax cabling through the open circuit, and the parasitic capacitance through its junction connection to the alligator clips. Measurements of the capacitance through the open circuit also account for the input impedance (25pF, 100Ω) of the amplifier. Measured capacitance for each resistor ranged from 35-55pF.

3.2. Shot Noise

The shot noise circuit circuit in Figure 2 features a 0.3μF DC–blocking capacitor (high-pass filter at 100Hz) and an op-amp network with a nominal gain of 10. The voltage noise from this network is connected to the same amplifier stage (Figure 1) discussed previously. Frequency gain of the amplification chain was characterized at nominal gains of 1000 and 2000 by disconnecting the photodiode and logarithmically sweeping a function generator through a test-input and measuring the RMS voltage from the second-stage output. As before, the photodiode and pre-amplifier stage were shielded and operated in battery mode to minimize background voltage noise.

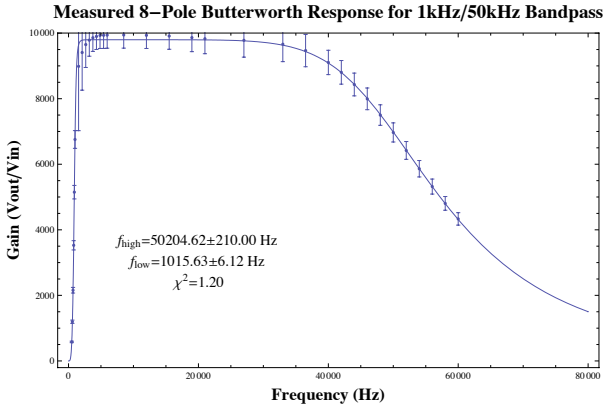

FIG. 3: Gain calibration for 1kHz–50kHz bandpass filter. The discrepancy from theory in the low-pass frequency rise is attributed to manufacturer-specified 0.1dB error.

Background noise was subtracted off in quadrature from measured photodiode voltage. For a 450kΩ resistor at a nominal gain of 2000, background noise was approximately 160mV$_{\mathrm{RMS}}$ and extrapolated shot-noise signal ranged between 2-20mV$_{\mathrm{RMS}}$. A fluctuating 1-5mV noise was observed for these measurements, suggesting either a resolution limitation at the digitizer, instability from measuring light bulb current in its transition region, instability in alkaline batteries as a power source, or extraneous noise from the amplifier and ambient electrical interference.

4. RESULTS AND ERROR ANALYSIS

Time variation of measurements, instrument uncertainty, repeatability, and the inherent statistical randomness of our measured processes contribute to systematic and random uncertainty in our error analysis for these measurements. Johnson and shot noise are moments of a random process of the electron. In the context of this process, error is negligible, as the digitizer in the amplification chain ensemble averages over massive sample sets (see caption of Figure 1). Uncertainty in voltage (σ_{V}), capacitance (σ_{C}), and resistance (σ_{R}) measurements were approximately 0.01mV-0.05mV, 0.0005nF, and 0.05kΩ. Error in capacitance and resistance are largely instrumental and also account for time variation at low-temperature measurements. Temperature uncertainty (σ_{T}) was approximately 3.5–5.5K, owing to phase change in ambient media over the hour and the low-precision of the toluene thermometer. Lastly, the manufacturer of our bandpass filter specifies a 0.1dB function deviation (σ_{BP}) from theoretical behavior[5].

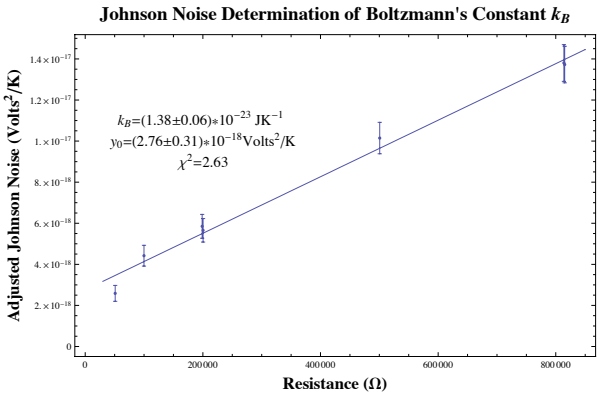

FIG. 4: Fit from adjusted Johnson noise and resistance.

4.1. Bandpass Filter Characterization

Johnson and shot noise are dependent on the frequency response and gain of our amplification chain, which we characterize here. The gain in our signal chain for a frequency $f = \omega/2\pi$ and amplifier gain A_0 is described by an 8-pole Butterworth response approximately between two corner frequencies f_{high} and f_{low}:

$$Y(f) = \frac{A_0}{\sqrt{1+\left(\frac{f_{\mathrm{high}}}{f}\right)^8}\sqrt{1+\left(\frac{f}{f_{\mathrm{low}}}\right)^8}} \tag{8}$$

Discounting resistive impedance in Equation 3, a plot of measured gain and its associated 8-pole Butterworth response is in Figure 3. Applying a Marquandt non-linear regression in Mathematica, the amplifier gain is well-characterized by Equation 8 ($\chi^2_\nu = 1.20$), and the corner frequencies are given by $f_{\mathrm{high}} = (50204.6 \pm 210.0)$Hz and $f_{\mathrm{low}} = (1015.63 \pm 6.12)$Hz. Equation 4 implies that equivalent noise bandwidth is determined by integrating over all frequencies. A real bandpass filter actually operates within its specified corner frequencies, therefore values of G used to determine k_B in the following are actually integrated from f_{high} to f_{low}. Integration errors negligible compared to other systematic errors.

Propagated errors the gain calibration are determined for the shot and Johnson measurements as,

$$\sigma_Y^2 = 4\left|Y(\omega)\right|^2\left(\frac{\sigma_{\mathrm{in}}^2}{V_{\mathrm{in}}^2}+\frac{\sigma_{\mathrm{out}}^2}{V_{\mathrm{out}}^2}\right)+\sigma_{\mathrm{BP}}^2, \tag{9}$$

$$\sigma_G^2 = 4\left(\frac{\left|Y(\omega)\right|^2}{1+(\omega R_0 C)^2}\right)^2\left(\frac{\sigma_{Y^2}^2}{Y^4}+\frac{\sigma_R^2}{R^2}+\frac{\sigma_C^2}{C^2}\right). \tag{10}$$

4.2. Measurement of Boltzmann Constant k_B and Absolute Zero

Figure 4 shows the results of plotting $\langle V^2\rangle/4TG$ against R_0, from whose slope we can determine k_B. Errors from voltage measurements of noise and shorted

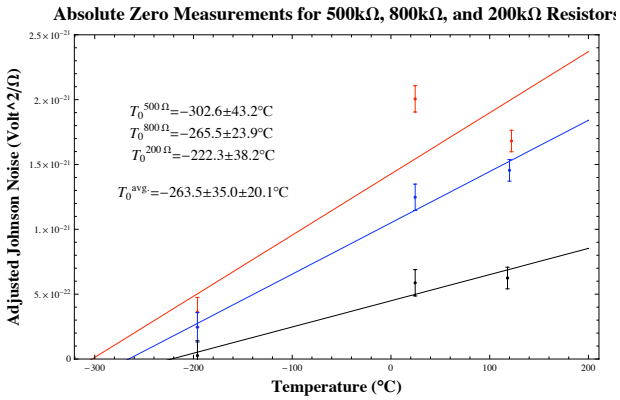

FIG. 5: Fit from adjusted Johnson noise and temperature.

noise add in quadrature to $\sigma^2_{\langle V^2\rangle}$

$$\sigma^2_{\frac{\langle V^2\rangle}{4GT}} = \left(\frac{\langle V^2\rangle}{4GT}\right)^2 \left(\frac{\sigma^2_{\langle V^2\rangle}}{\langle V^2\rangle^2} + \frac{\sigma_T^2}{T^2} + \frac{\sigma_G^2}{G^2}\right). \qquad (11)$$

The experimentally determined value is Boltmann's constant is $k_B = (1.38 \pm 0.06) \times 10^{-23}\mathrm{J}\cdot\mathrm{K}^{-1}$, which agrees excellently with the accepted NIST value of $1.3806504(24) \times 10^{-23}\mathrm{J}\cdot\mathrm{K}^{-1}$ [6]. We expect that our fit line ($\chi^2_\nu = 2.63$) to have a y-intercept at 0 from Equation 7, however our measured y-intercept is given by $(2.76 \pm 0.31) \times 10^{-18}\mathrm{Volts}^2/\mathrm{K}$, which indicates that additional background voltage noise may not be accounted for the quadrature interpolation of Johnson noise, and that additional sources of noise (Johnson and shot noise) may be correlated. Furthermore, note that 50kΩ outlier may be attributed to an impedance mismatch between the source resistor, amplifier, and coax cabling.

Figure 5 shows the results of plotting $\langle V^2\rangle/4RG$ against T for three resistors theoretically valued at 200kΩ, 500kΩ, and 800kΩ, from whose y-intercept we can determine T_0. Error from these points is calculated similarly to Equation 11. Averaging the intercepts for the three resistors, our experimentally determined value of absolute zero is $T_0 = (-263.49 \pm 35.0 \pm 20.2)^\circ C$, which agrees within experimental error of the accepted value $T_0 = -273.15K$ [6]. As only three points are used for each of these points, a χ^2 test of confidence is omitted.

Note that a non-equilibrium temperature gradient between a resistor and the ambient environment may result in a departure from the linear temperature dependence of Johnson noise as predicted by Nyquist's theorem. For this reason, systematic error for each of our measurements is larger than it would had it been possible to take measurements thermally coupled to each resistor. As temperature increases, it is more likely for the resistor to approach thermal equilibrium with radiating metal surfaces around it, such as the surface of the oven or the alligator clips, and have an empirical temperature consistently higher than the ambient temperature being measured. Our noise measurements likely overestimated the actual Johnson noise across each resistor for a given temperature.

4.3. Shot Noise Determination of Electron Charge

To determine shot noise, we plot the adjusted shot-noise voltage V/R_fG against photoelectric voltage for a nominal gain of 1000 (χ^2_ν =1.32) and 2000 (χ^2_ν =1.93), determining the electron charge to $e = (1.48 \pm 0.05) \cdot 10^{-19}$C and $e = (1.59 \pm 0.08) \cdot 10^{-19}$C. Repeated measurements of the 1000 gain measurement yielded consistently low values of e, suggesting that fluctuating background noise may be comparable in magnitude to our amplified shot-noise signal. Our measured value with 2000 gain is in excellent agreement with the accepted value of $1.602176487(40)\times10^{-23}$C[6].

5. CONCLUSIONS

In summary, we have measured Boltzmann's constant, absolute zero, and the charge of the electron to within experimental error, thereby validating Nyquist's theory of voltage noise from thermal motion of electrons and their quantization. The frequency-response of the amplification chain used in this measurement was a well-characterized Butterworth transfer function.

Our method indicates a number of improvements that future students could make in order to obtain more accurate data. First, measuring shunt and parasitic capacitance should take into account capacitance inherent to the setup as well as that due to the resistor and its junction connection to the test box. Second, measuring the temperature in a thermally-coupled manner without introducing line noise or capacitive coupling is a hurdle that should be addressed. Non-equilibrium behavior of resistors will likely cause actual values of noise to be higher for a measured temperature. Three simple solutions would mitigate these difficulties: first, the use of a conductive platinum resistance thermometer; second, the addition of a thermally stable oil (dibutyl phthalate, paraffin wax, or silicone oil) to a heat bath; and third, to vacuum pump air out of the oven and allow only for thermal transfer between the resistor and oven surface.

Acknowledgments

B. Mookerji thanks C. Herder for his equal contribution to the this experiment and its analysis, and the Junior Lab staff.

[1] P. Horowitz and W. Hill, *The Art of Electronics* (Cambridge University Press, 1989).

[2] J. L. Staff, *Johnson and Shot Noise Lab Guide* (8.13,

2007).
[3] F. Reif, *Fundamentals of Statistical and Thermal Physics* (McGraw-Hill, 1965).
[4] W. H. P. Kittel and R. Donnelly, Am. J. Phys. **46**, 94 (1977).
[5] Khron-Hite, *3BS8TB-1k/50kg 1kHz–50kHz BandPass Data Sheet (https//web.mit.edu/8.13/)* (????).
[6] (????), URL http://nist.gov.